
# Ferromagnetic Heisenberg spin chain in a resonator

Yusong Cao(曹雨松), Junpeng Cao(曹俊鹏), and Heng Fan(范桁)

**Citation:**Chin. Phys. B, 2021, 30 (**9**): 090506. DOI: 10.1088/1674-1056/ac1334
Journal homepage: http://cpb.iphy.ac.cn; http://iopscience.iop.org/cpb

**What follows is a list of articles you may be interested in**

---

## Equilibrium dynamics of the sub-ohmic spin-boson model at finite temperature

Ke Yang(杨珂) and Ning-Hua Tong(同宁华)
Chin. Phys. B, 2021, 30 (**4**): 040501. DOI: 10.1088/1674-1056/abd393

## Quantum dynamics on a lossy non-Hermitian lattice

Li Wang(王利), Qing Liu(刘青), and Yunbo Zhang(张云波)
Chin. Phys. B, 2021, 30 (**2**): 020506. DOI: 10.1088/1674-1056/abd765

## Entangled multi-knot lattice model of anyon current

Tieyan Si(司铁岩)
Chin. Phys. B, 2019, 28 (**4**): 040501. DOI: 10.1088/1674-1056/28/4/040501

## Dynamical correlation functions of the quadratic coupling spin-Boson model

Da-Chuan Zheng(郑大川), Ning-Hua Tong(同宁华)
Chin. Phys. B, 2017, 26 (**6**): 060502. DOI: 10.1088/1674-1056/26/6/060502

## Chaos in a fractional-order micro-electro-mechanical resonator and its suppression

Mohammad Pourmahmood Aghababa
Chin. Phys. B, 2012, 21 (**10**): 100505. DOI: 10.1088/1674-1056/21/10/100505

---

# Ferromagnetic Heisenberg spin chain in a resonator

Yusong Cao(曹雨松)[1,2,†], Junpeng Cao(曹俊鹏)[1,2,3,4], and Heng Fan(范桁)[1,2,3,5]

[1] *Beijing National Laboratory for Condensed Matter Physics, Institute of Physics, Chinese Academy of Sciences, Beijing* 100190, *China*
[2] *School of Physical Sciences, University of Chinese Academy of Sciences, Beijing* 100049, *China*
[3] *Songshan Lake Materials Laboratory, Dongguan* 523808, *China*
[4] *Peng Huanwu Center for Fundamental Theory, Xi'an* 710127, *China*
[5] *CAS Center for Excellence in Topological Quantum Computation, University of Chinese Academy of Sciences, Beijing* 100190, *China*

(Received 1 May 2021; revised manuscript received 6 July 2021; accepted manuscript online 12 July 2021)

We investigate the properties of a generalized Rabi model by replacing the two-level atom in Rabi model with a ferromagnetic Heisenberg spin chain. We find that the dynamical behavior of the system can be divided into four categories. The energy spectrum of the ground state and some low excited states are obtained. When the magnons and the photon are in resonance, the model is exactly solvable and the rigorous solution is obtained. Near the resonance point where the detuning is small, the system is studied with the help of perturbation theory. This model has a spontaneously breaking of parity symmetry, suggesting the existence of a quantum phase transition. The critical exponent from the normal phase is computed.

**Keywords:** magnon, resonator, quantum phase transition

**PACS:** 05.30.Jp, 03.67.Lx, 42.50.–p **DOI:** 10.1088/1674-1056/ac1334

## 1. Introduction

Rabi model plays an important role in various fields in physics. The physical setup of the Rabi model is very simple: a two-level atom with magnetic momentum and electrical dipole momentum in an electromagnetic resonator.[1] One of the reasons that Rabi model draws so much attention is the rich experimental realizations of the two-level systems such as the quantum qubit in quantum computation.[2–6] Rabi model also plays an important role in the semiconductor physics[7] and the ion-trap technology.[8] In the quantum technology, especially the quantum information and quantum computation, we need many two-level systems to serve as quantum gates to perform quantum computing. One of the associated models is the Dicke model which is a generalization of Rabi model.[9] The Dicke model describes $N$ free two-level atoms interacting with the cavity field. We should note that the behavior of the photon field is also worth studying. The most representative example is the superradiant phase transition of the cavity field obtained from the thermodynamical limit of the Dicke model. This kind of phase transition belongs to the quantum phase transition.[10–16]

Recently, the application of Rabi model and generalized Rabi models in the condensed matter physics causes renewed interests and has been studied extensively.[17–21] The typical Rabi-type model is the Rabi–Hubbard model, where the two-level atom is replaced by a Hubbard lattice.

When the two-level systems are used to simulate the quantum qubits in the cavity QED experiments, the decoherence of the qubit systems is a major problem which may cause the trouble in building the quantum gates. In order to overcome this difficulty, one possible scheme is to search for different carriers of quantum qubits such as the superconductor qubits, annoys qubits, and magnon qubits in the ferromagnets.[22–29]

In this paper, we consider the ferromagnetic Heisenberg spin chain in a resonator. The system is obtained by replacing the two-level atom in the Rabi model by the spin chain with ferromagnetic isotropic nearest neighbor exchanging interactions. The elementary excitation of the spin chain is the magnon. The magnons interact with the electromagnetic field in the resonator. We find that the dynamical behavior of the system can be divided into four regimes, i.e., decoupling regime, Jaynes–Cummings (JC) regime, two-fold dispersive regime, and ultra-strong coupling regime, based on the oscillation frequencies of different interaction terms. We obtain the energy spectrum of the ground state and low excited states of the system. If the magnons and cavity field modes are in resonance, we obtain the analytical solution of the system. Near the resonance point where the detuning is very small, we study the system with the perturbation theory. We also discuss the symmetry broken of the system. We find that the cavity field exhibits a quantum phase transition. The corresponding critical exponent from normal phase is given.

This paper is organized as follows. We introduce the Hamiltonian of the system in Section 2. In Section 3, we compute the energy spectrum at the ground state and the low excited states in different regimes of model parameters by using the different methods such as exact solution, effective Hamil-

†Corresponding author. E-mail: caoyusong15@mails.ucas.ac.cn

 

tonian, and perturbation theory. In Section 4, we discuss the symmetry broken of the system and give the critical exponent of the quantum phase transition. The main results are summarized in Section 5.

## 2. Model Hamiltonian

The model considered in this paper contains three parts: (a) a spin chain with ferromagnetic isotropic nearest neighbor interaction, (b) a resonator with electromagnetic field, and (c) interaction between the spin chain and the electromagnetic field. The model Hamiltonian reads $H_{\rm m} = H_{\rm FM} + H_{\rm EM} + H_{\rm int}$. Here the $H_{\rm FM}$ denotes the Hamiltonian of the ferromagnetic Heisenberg spin chain

$$H_{\rm FM} = -J\sum_{j=1}^{N} \boldsymbol{S}_j \cdot \boldsymbol{S}_{j+1}, \tag{1}$$

where $J$ is the coupling constant, $N$ is the number of sites, and $\boldsymbol{S}_j$ is the spin-$S$ operator at site $j$. We consider the periodic boundary condition thus $\boldsymbol{S}_{N+1} = \boldsymbol{S}_1$. The term $H_{\rm EM}$ stands for the Hamiltonian of the electromagnetic field in the resonator

$$H_{\rm EM} = \frac{1}{2}\int {\rm d}V \left(\varepsilon \boldsymbol{E}^2 + \frac{\boldsymbol{B}^2}{\mu}\right), \tag{2}$$

where $\varepsilon$ is the electrical conductivity, $\mu$ is the magnetic conductivity, and $\boldsymbol{E}$ and $\boldsymbol{B}$ are the strengths of electric field and magnetic field, respectively. The term $H_{\rm int}$ is resulted from the interaction between the spins and the magnetic field in the resonator

$$H_{\rm int} = \frac{g}{\mu}\sum_{j=1}^{N} \boldsymbol{S}_j \cdot \boldsymbol{B}(\boldsymbol{x}_j), \tag{3}$$

where $g$ is the coupling constant and $\boldsymbol{x}_j$ is the position of the $j$-th spin.

In order to see the collective behavior of the spin chain more clearly, we write the Hamiltonian $H_{\rm m}$ in the momentum representation. With the help of Holstein–Primakoff transformation, if the spin $S$ is large enough and the chain is in the low excited states, the Hamiltonian of the spin chain ($\hbar = 1$) reads

$$H_{\rm FM} = \sum_{k=-\infty}^{\infty} \Omega_k b_k^\dagger b_k, \tag{4}$$

where $\Omega_k$ is the dispersion function of the magnons, and $b_k$ and $b_k^\dagger$ are the annihilation and creation operators of the magnon with wave vector $k$, respectively. The Hamiltonian of the electromagnetic field in momentum representation reads

$$H_{\rm EM} = \sum_{k>0} \omega_k a_k^\dagger a_k, \tag{5}$$

where $\omega_k$ is the dispersion function of the photons, and $a_k$ and $a_k^\dagger$ are the annihilation and creation operators of the photon with mode $k$, respectively. Now, we shall deal with the interaction term. For convenience, we consider the thermodynamic limit where $N$ tends to infinity. We put the spin chain and the standing electromagnetic wave on the $z$ direction. The magnetic field is along the $y$-axis

$$B_y(z) = -{\rm i}\varepsilon c\sum_{k>0} \varepsilon_k (a_k - a_k^\dagger)\cos kz, \tag{6}$$

where $c$ is the light speed, $\varepsilon_k = \frac{\omega_k}{\varepsilon V}$, and $V$ is the volume of the resonator. Then the interaction term can be written as

$$\begin{aligned} H_{\rm int} &= g\sum_{j=1}^{N} S_j^y B_y(z_j) \\ &= -\frac{g\varepsilon_0 c}{4}\sqrt{2SN}\sum_{k>0} \varepsilon_k [(b_k - b_k^\dagger)(a_k - a_k^\dagger) \\ &\quad + (b_{-k} - b_{-k}^\dagger)(a_k - a_k^\dagger)], \end{aligned} \tag{7}$$

In the derivation, we have used the relation $\frac{1}{N}\sum_l {\rm e}^{{\rm i}(k-k')x_l} = \delta_{k,k'}$. We further define $g_k = -\frac{g\varepsilon c}{4}\sqrt{2SN}\varepsilon_k$. Then the interaction term takes the form of

$$\begin{aligned} H_{\rm int} &= \sum_{k>0} g_k [(b_k - b_k^\dagger)(a_k - a_k^\dagger) \\ &\quad + (b_{-k} - b_{-k}^\dagger)(a_k - a_k^\dagger)]. \end{aligned} \tag{8}$$

Next, we write the full Hamiltonian as $H_{\rm m} = H_1 + H_2$, where

$$\begin{aligned} H_1 &= \sum_{k>0} [\Omega_k b_k^\dagger b_k + \omega_k a_k^\dagger a_k + g_k [(b_k - b_k^\dagger)(a_k - a_k^\dagger)], \\ H_2 &= \sum_{k>0} [\Omega_{-k} b_{-k}^\dagger b_{-k} + \omega_k a_k^\dagger a_k \\ &\quad + g_k [(b_{-k} - b_{-k}^\dagger)(a_k - a_k^\dagger)]. \end{aligned} \tag{9}$$

From Eq. (9), we know that the Hamiltonian $H_1$ is blocked in momentum space, i.e., $H_1 = \sum_k H_{1,k}$, because the magnon with wave vector $k$ only interacts with the photon of mode $k$. The explicit form of $H_{1,k}$ reads

$$H_{1,k} = \Omega_k b_k^\dagger b_k + \omega_k a_k^\dagger a_k + g_k [(b_k - b_k^\dagger)(a_k - a_k^\dagger)]. \tag{10}$$

We should note that the Hamiltonian $H_1$ acts only on the Hilbert space with magnon vector $k > 0$. In the Hamiltonian $H_2$, the magnon with wave vector $-k$ only interacts with the photon of mode $k$. Thus $H_2$ acts on the Hilbert space with magnon wave vector $k < 0$. In the experiment settings, we could use external methods to modulate the magnons. For example, by putting a spin wave valve on the spin chain, we can get rid of all the magnons with wave vector $k < 0$, which allows us to eliminate the term $H_2$ and only consider the Hamiltonian $H_1$.

We concentrate on the Hamiltonian $H_{1,k}$. Omitting the subscripts, we arrive at

$$H = \omega a^\dagger a + \Omega b^\dagger b + g(a - a^\dagger)(b - b^\dagger). \tag{11}$$

For the later using, we rewrite Hamiltonian (11) as $H = H_0 + H_{\rm I}$, where $H_0 = \omega a^\dagger a + \Omega b^\dagger b$ denotes the non-interacting parts and $H_{\rm I} = g(a - a^\dagger)(b - b^\dagger)$ means the interaction terms. Comparing with the standard Rabi model, we find that the $H_{\rm I}$ can also be rewritten as

$$H_{\rm I} = H_{\rm cr} - H_{\rm r}, \tag{12}$$

where $H_{\rm r} = g(a^\dagger b + a b^\dagger)$ and $H_{\rm cr} = g(a^\dagger b^\dagger + ab)$ are the rotating wave and counter-rotating wave terms, respectively.

## 3. Dynamics and solutions

In order to study the dynamic behavior of the system (11), we first consider the interaction term $H_{\rm I}$ in the interaction picture

$$\begin{aligned} H_{\rm I}(t) &= {\rm e}^{{\rm i}H_0 t} H_{\rm I} {\rm e}^{-{\rm i}H_0 t} \\ &= g[{\rm e}^{-{\rm i}(\omega+\Omega)t} ba + {\rm e}^{{\rm i}(\omega+\Omega)t} b^\dagger a^\dagger \\ &\quad + {\rm e}^{-{\rm i}(\omega-\Omega)t} ba^\dagger - {\rm e}^{{\rm i}(\omega+\Omega)t} b^\dagger a]. \end{aligned} \tag{13}$$

From Eq. (13), we see that the rotating wave term and counter-rotating wave term oscillate with different frequencies, which is similar to the case of Rabi model.[30] Because the different interaction terms oscillate with different frequencies, the oscillating terms with high frequencies can be neglected. From the detailed analysis of Eq. (13), we find that the dynamical behavior of the Hamiltonian (11) can be divided into following four regimes of model parameters: (i) decoupling regime where $g \ll \omega$ and $g \ll \Omega$; (ii) JC regime where $g \ll \omega$, $g \ll \Omega$ and $|\omega - \Omega| \ll |\omega + \Omega|$; (iii) two-fold dispersive regime where $g < \omega$, $g < \Omega$, $g < |\omega - \Omega|$ and $g < |\omega + \Omega|$; (iv) ultra-strong coupling regime where $g > \omega$ and $g > \Omega$.

We shall note that the dynamical properties of Hamiltonian (11) and those of Rabi model[30] are different. First, in the Hamiltonian (11), there is no electrical dipole momentum. It is the magnetic momentum interacting with the magnetic field, which induces both the rotating wave and the counter-rotating terms. The Zeeman term in the Rabi model is replaced by the kinetic energy term of the magnons. Second, the rotating wave and counter-rotating wave terms in the Hamiltonian (11) always have opposite signs. Third, in the present system (11), there does not exist the anti-JC regime of the Rabi model because the constraint $|\omega - \Omega| > |\omega + \Omega|$ of anti-JC regime cannot be achieved by the present requirements $\omega > 0$ and $\Omega > 0$.

In the following subsections, we solve the eigen-energy spectrum of system (11). We focus on the later three regimes because there is no interaction in the decoupling regime and the corresponding results are direct.

### 3.1. JC regime

In the JC regime, the contour-rotating wave term can be neglected, i.e., $H_{\rm cr} = 0$. Then the particle number operator $\hat{N} = a^\dagger a + b^\dagger b$ of the system is conserved. This means that the Hamiltonian (11) is blocked as $H = \oplus_n H_n$, where $n$ is the particle number that is the eiegenvaue of $\hat{N}$ and $H_n$ is a $(n+1) \times (n+1)$ matrix with the form of

$$H_n = \begin{pmatrix} n\omega & -g\sqrt{n} & 0 & \cdots & 0 & 0 \\ -g\sqrt{n} & (n-1)\omega + \Omega & -g\sqrt{2(n-1)} & \cdots & 0 & 0 \\ 0 & -g\sqrt{2(n-1)} & (n-2)\omega + 2\Omega & \cdots & 0 & 0 \\ 0 & 0 & \cdots & \cdots & -g\sqrt{2(n-1)} & 0 \\ 0 & 0 & \cdots & -g\sqrt{2(n-1)} & \omega + (n-1)\Omega & -g\sqrt{n} \\ 0 & 0 & \cdots & 0 & -g\sqrt{n} & n\Omega \end{pmatrix}. \tag{14}$$

We see that the $H_n$ is a tridiagonal matric which can be diagonalized numerically for arbitrary particle number $n$. If the particle number $n$ is small, we can obtain the analytical results.

The Hamiltonian (11) in the JC regime reads $H = H_0 + H_{\rm r}$, where $H_0$ is diagonal. Thus if the coupling constant $g$ in $H_{\rm r}$ is small, we can also solve the $H$ by using the perturbation theory. In Fig. 1, we show the energy spectrum of Hamiltonian (11) at the ground state and the first two excited states as the functions of $g$. The dots are the results obtained by the exact diagonalization of the Hamiltonian (11), while the solid lines are those obtained by using the perturbation theory up to the second order. We see that they are consistent with each other very well if the coupling strength $g$ is small. This result is in agreement with that the perturbation theory is more accurate when the perturbation parameter is small. From Eq. (14), we see that the first two excited state energies can also be obtained by diagonalizing the matrix (14) in the subspace with $n = 1$. The results are shown in Fig. 2, where the dots are the energy spectrum at the ground state and the first two excited states obtained by exact diagonalization of the blocked Hamiltonian (14) and the lines denotes the corresponding results obtained by using the perturbation theory. Again, they are consistent with each other very well if the coupling strength $g$ is small.

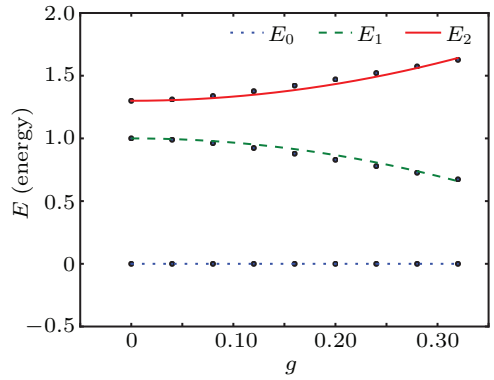


**Fig. 1.** The energy spectrum of the system (11) in the JC regime at the ground state and the first two excited states as the functions of $g$. The dots are the results obtained by the exact diagonalization of the Hamiltonian (11), while the solid lines are those obtained by using the perturbation theory. We see that they are consistent with each other very well if the coupling strength $g$ is small. Here $\omega = 1$ and $\Omega = 1.3$. In the simulation, the dimensions of operator $a$ and $b$ are $200 \times 200$ and $10 \times 10$, respectively.

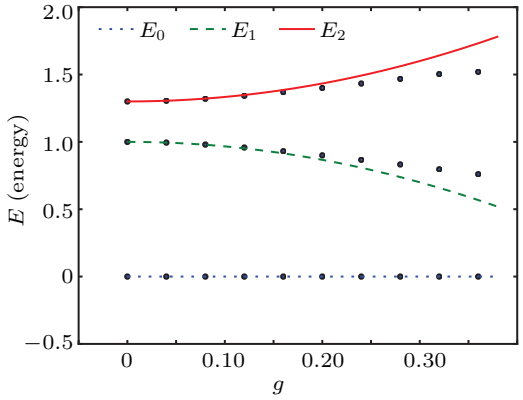


**Fig. 2.** The energy spectrum of the system at the ground state and the first two excited states in JC regime as the functions of $g$. The dots are the results obtained from the diagonalization of block Hamiltonian (14) with $n = 0, 1$. The solid lines are the results obtained from the perturbation theory. We have set $\omega = 1$ and $\Omega = 1.3$.

### 3.2. Two-fold dispersive regime

In the most experiments, the tunable parameters are in the two-fold dispersive regime. Since there is no analytic solution in this regime, we should solve the Hamiltonian with the help of numerical or approximation methods. From the above analysis, we know that the coupling strength $g$ in this regime is small, which means that we can study the second order effective Hamiltonian just like the case in Rabi model.[31] In the language of scattering theory, the particle numbers of both photon and magnon are conserved in the scattering process. In order to obtain the effective Hamiltonian, we examine the matric elements

$$\langle n_a, n_b | H_{\rm I}^r | n_a, n_b \rangle, \tag{15}$$

where $r$ is a positive integer, $n_a$ and $n_b$ are the particle numbers of photon and magnon, respectively. We see that the relation $r \geq 2$ must hold if the matric element (15) is required to be non zero. Therefore, up to the second order of $g$, the effective Hamiltonian of the system reads

$$H_{\rm eff} = (\omega + g)a^\dagger a + (\Omega + g)b^\dagger b + g^2 b^\dagger b a^\dagger a. \tag{16}$$

From Eq. (16), we see that the effective Hamiltonian $H_{\rm eff}$ is a diagonal matrix and the diagonal elements in the particle number representation are the eigenvalues.

In Fig. 3, we show the ground state and the first two excited states energies of the system obtained by using the exact diagonalization of the Hamiltonian and by the effective Hamiltonian method. We see that the results are consistent with each other when $g$ is small.

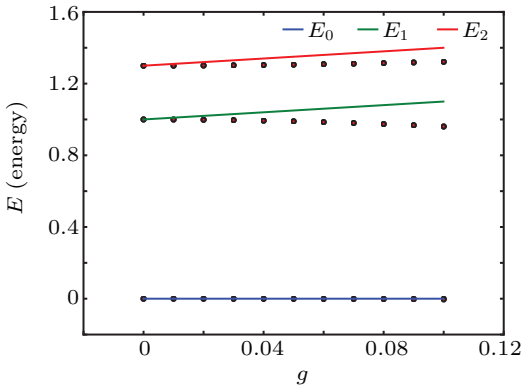


**Fig. 3.** The energy spectrum for the ground state and the first two excited states in the two-fold dispersive regime. The dots are the results obtained from exact diagonalization of the Hamiltonian. The solid lines are the results obtained from the effective Hamiltonian. We have set $\omega = 1$ and $\Omega = 1.3$.

### 3.3. Ultra-strong coupling regime

#### 3.3.1. Analytical point

In the ultra-strong coupling regime, the coupling constant $g$ is large and we can not take the perturbation to $g$. We discuss the system in the resonance point of $\omega = \Omega$, where the Hamiltonian (11) reads

$$H = \omega a^\dagger a + \omega b^\dagger b + g(b - b^\dagger)(a - a^\dagger). \tag{17}$$

The Hamiltonian (17) is exactly solvable. Define the position-representations of the two sets of boson operators as

$$\begin{aligned} x &= \frac{1}{\sqrt{2\omega}}(a + a^\dagger), \quad y = \frac{1}{\sqrt{2\omega}}(b + b^\dagger), \\ p_x &= {\rm i}\sqrt{\frac{\omega}{2}}(a - a^\dagger), \quad p_y = {\rm i}\sqrt{\frac{\omega}{2}}(b - b^\dagger). \end{aligned} \tag{18}$$

Then the Hamiltonian (17) becomes

$$H = \frac{p_x^2}{2} + \frac{p_y^2}{2} - \frac{g\omega}{2}p_x p_y + \frac{\omega^2}{2}(x^2 + y^2). \tag{19}$$

With the help of rotations of coordinate

$$\begin{aligned} x_- &= \frac{1}{\sqrt{2}}(x + y), \quad x_+ = \frac{1}{\sqrt{2}}(x - y), \\ p_- &= \frac{1}{\sqrt{2}}(p_x + p_y), \quad p_+ = \frac{1}{\sqrt{2}}(p_x - p_y), \end{aligned} \tag{20}$$

the Hamiltonian (19) turns into

$$H = \sum_{j=\pm} \lambda_j \left( \frac{p_j^2}{2} + \frac{\omega^2 x_j^2}{2\lambda_j} \right), \tag{21}$$

where

$$\lambda_+ = 1+\frac{g\omega}{2}, \quad \lambda_- = 1-\frac{g\omega}{2}. \tag{22}$$

We define a new pair of creation and annihilation operators

$$a_j^\dagger = \sqrt{\frac{\omega_j}{2}}\left(x_j+\frac{\mathrm{i}p_j}{\omega}\right), \ a_j = \sqrt{\frac{\omega_j}{2}}\left(x_j-\frac{\mathrm{i}p_j}{\omega}\right), \ j=\pm. \tag{23}$$

Then the energy spectrum of Hamiltonian (21) is

$$E_{n_+,n_-} = \sum_{j=\pm}\lambda_j\omega_j\left(n_j+\frac{1}{2}\right), \tag{24}$$

where $\omega_\pm = \omega/\sqrt{1\pm g\omega/2}$. In Fig. 4, we show the energy spectrum of the ground state and the first two excited states as the functions of $g$. We see that there is a level crossing between the ground state and the first excited state at the point of $g_l = 4\sqrt{1+2\omega^2}-2(1+2\omega^2)/\omega$. Therefore, if $g<g_l$, the ground state wave function is

$$\psi(x_+,x_-) = \left(\frac{\omega_+\omega_-}{\pi^2}\right)^{\frac{1}{4}}\exp\left(-\frac{\omega_+x_+^2}{2}-\frac{\omega_-x_-^2}{2}\right).$$

While if $g>g_l$, the ground wave function is

$$\psi(x_+,x_-) = \sqrt{2}\left(\frac{\omega_+\omega_-^3}{\pi^2}\right)^{\frac{1}{4}}x_-\exp\left(-\frac{\omega_+x_+^2}{2}-\frac{\omega_-x_-^2}{2}\right).$$

Last, we should note that the above treatment method of resonance case is valid in all the regimes of model parameters.

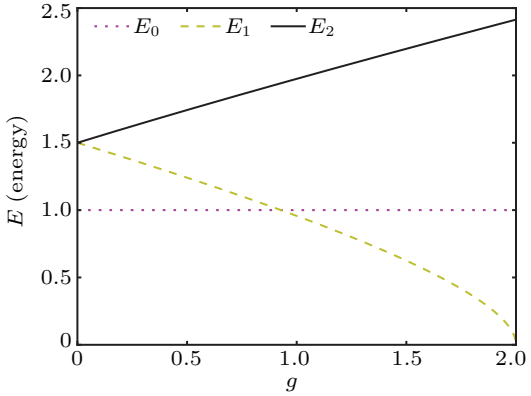


**Fig. 4.** The energy spectrum for the ground state and the first two excited states as the functions of $g$ at the resonance point $\omega=\Omega$. We find that there exists a level crossing of energies at the ground state and the first excited state, resulting in the changing of parity of the ground state wave functions. We have set $\omega=\Omega=1$.

### 3.3.2. Detuning

Next, we consider the regime near the resonance point. We define the detuning factor $\delta$ as $\Omega=\omega+\delta$. Then the Hamiltonian (11) reads

$$H = \omega a^\dagger a+(\omega+\delta)b^\dagger b+g(b-b^\dagger)(a-a^\dagger). \tag{25}$$

Substituting Eqs. (18), (20), and (23) into the above Hamiltonian, we arrive at

$$\begin{aligned} H &= \sum_{j=\pm}\lambda_j\left(\frac{p_j^2}{2}+\frac{\omega_j^2x_j^2}{2}\right) \\ &\quad +\delta\left[\frac{1}{4}(p_- - p_+)^2+\frac{\omega^2}{4}(x_- - x_+)^2\right] \\ &= \sum_{j=\pm}\lambda_j\omega_j a_j^\dagger a_j+\frac{\delta}{4}\left[\left(\frac{\omega}{2\omega_-}-\frac{\omega_-}{2}\right)(a_-^\dagger - a_-)^2\right. \\ &\quad +\left(\frac{\omega}{2\omega_+}-\frac{\omega_+}{2}\right)(a_+^\dagger - a_+)^2 \\ &\quad \left.+\left(\sqrt{\omega_-\omega_+}-\sqrt{\frac{\omega^2}{\omega_-\omega_+}}\right)(a_-^\dagger - a_-)(a_+^\dagger - a_+)\right]. \end{aligned} \tag{26}$$

Rewrite the Hamiltonian (26) as $H=H_a+H_p$, where $H_a$ stands for the resonance Hamiltonian given by Eq. (17) and $H_p$ stands for the extra terms as a result of detuning

$$\begin{aligned} H_p &= \frac{\delta}{4}\left[\left(\frac{\omega}{2\omega_-}-\frac{\omega_-}{2}\right)(a_-^\dagger - a_-)^2\right. \\ &\quad +\left(\frac{\omega}{2\omega_+}-\frac{\omega_+}{2}\right)(a_+^\dagger - a_+)^2 \\ &\quad \left.+\left(\sqrt{\omega_-\omega_+}-\sqrt{\frac{\omega^2}{\omega_-\omega_+}}\right)(a_-^\dagger - a_-)(a_+^\dagger - a_+)\right]. \end{aligned} \tag{27}$$

Since $H_a$ has been solved exactly and the detuning factor $\delta$ is small, we can treat $H_p$ as the perturbation. Up to the first order of $\delta$, the energy shifts of the first three eigen-energies of the Hamiltonian (26) are

$$\Delta E_0 = \frac{\delta}{4}\left(\frac{\omega_+ + \omega_-}{2}-\frac{\omega}{2\omega_+}-\frac{\omega}{2\omega_-}\right), \tag{28}$$

$$\Delta E_+ = \frac{\delta}{4}\left(\frac{3\omega_+ + \omega_-}{2}-\frac{3\omega}{2\omega_+}-\frac{\omega}{2\omega_-}\right), \tag{29}$$

$$\Delta E_- = \frac{\delta}{4}\left(\frac{\omega_+ + 3\omega_-}{2}-\frac{\omega}{2\omega_+}-\frac{3\omega}{2\omega_-}\right). \tag{30}$$

From Eq. (28), we see that the level crossing of the ground state and the first excited state takes place at

$$\frac{\delta^2}{16}(\lambda_- - \omega)^2 = \omega^2\lambda_-^3. \tag{31}$$

## 4. Symmetry-broken and quantum phase transition

The Hamiltonian (11) possesses the $Z_2$ symmetry induced by parity operator $P=\exp[\mathrm{i}\pi(a^\dagger a+b^\dagger b)]$. With the help of Baker–Housedorff equation, we have

$$\begin{aligned} &P^{-1}aP = -a, \quad P^{-1}a^\dagger P = -a^\dagger, \\ &P^{-1}bP = -b, \quad P^{-1}b^\dagger P = -b^\dagger. \end{aligned} \tag{32}$$

Thus the Hamiltonian (11) can be divided into $H=H^{(+)}\oplus H^{(-)}$, where the superscripts are the quantum number of parity operator. In the resonance case $\omega=\Omega$, we have

$$H^{(j)} = \lambda_j\left(a_j^\dagger a_j+\frac{1}{2}\right), \quad j=\pm. \tag{33}$$

From Eq. (22), we know that $\lambda_-$ vanishes at the point of $g_c = 2/\omega$, which means that if $g > g_c$, there does not exist the subspace with negative parity. The $Z_2$ symmetry is broken spontaneously, which results in the phase transition of the photon field. Near the critical point $g_c$, the frequency $\omega_-$ with negative parity is

$$\omega_-(g\to g_c) = \frac{\omega}{\sqrt{1-\frac{g\omega}{2}}} = \frac{2}{\sqrt{g_c^2 - g g_c}} \sim |g_c - g|^{-\frac{1}{2}}. \tag{34}$$

In order to obtain the critical exponent of the quantum phase transition, we apply the length scale method introduced in Ref. [16]. The characteristic length scale of the system (11) in terms of energy is defined as

$$l_- = \frac{1}{\sqrt{\omega_-}}. \tag{35}$$

From Eq. (34), we know that the characteristic length $l_-$ divergences as $|g_c - g|^{-1/2}$, which gives the critical exponent as $\nu = -1/4$.

## 5. Summary

In conclusion, we have studied the ferromagnetic Heisenberg spin chain in a resonator with spin wave valve. We find that the dynamical behavior of the system can be divided into four regimes according to the relation between the coupling strength and the frequencies of magnon and photon. We present the energy spectrum of the ground state and the first two excited sates in the JC and two-fold dispersive regimes. In the resonance case, we obtain the exact solutions of the system and the corresponding treatment method is universal, which can be applied to all the regimes of model parameters, especially in the ultra-strong coupling regime. Near the resonance point, we solve the system by using the perturbation method. Further, we analyze the spontaneous breaking of parity symmetry and study the critical exponent of quantum phase transition of the photon field from the normal phase.

## References


[1] Rabi I I 1937 *Phys. Rev.* **51** 652
[2] Raimond J M, Brune M and Haroche S 2001 *Rev. Mod. Phys.* **73** 565
[3] Liebfried D, Blatt R, Monroe C and Wineland D 2003 *Rev. Mod. Phys.* **75** 281
[4] Englund D, Faraon A, Fushman I, Stoltz N, Petroff P and Vuckovic J 2007 *Nature* **450** 857
[5] Cordero S, Nahmad-Achar E, Lopez-Pena R and Castanos O arXiv:2002.02491 [quant-ph]
[6] Shen L, Yang J, Shi Z, Zhong Z and Xu C 2021 *J. Phys. A: Math. Theor.* **54** 105302
[7] Khitrova G, Gibbs H M, Kira M, Koch S W and Scherer A 2006 *Nat. Phys.* **2** 81
[8] Leibfried D, Blatt R, Monroe C and Wineland D 2003 *Rev. Mod. Phys.* **75** 281
[9] Dicke R H 1954 *Phys. Rev.* **93** 99
[10] Hepp K and Lieb E H 1973 *Ann. Phys.* **76** 360
[11] Peng J, Rico E, Zhong J, Solano E and Egusquiza I L 2019 arXiv:1904.02118 [quant-ph]
[12] Ying Z, Cong L and Sun X 2020 *J. Phys. A: Math. Theor.* **53** 345301
[13] Liu M, Chesi S, Ying Z, Chen X, Luo H and Lin H 2017 *Phys. Rev. Lett.* **119** 220601
[14] Lambert N, Emary C and Brandes T 2005 *Phys. Rev. A* **71** 053804
[15] Lambert N, Emary C and Brandes T 2004 *Phys. Rev. Lett.* **92** 073602
[16] Emary C and Brandes T 2003 *Phys. Rev. E* **67** 066203
[17] Flottat T, Hebert F, Rousseau V G and Batrouni G G 2016 *Eur. Phys. J. D* **70** 213
[18] Schiro M, Bordyuh M, Oztop B and Tureci H E 2013 *J. Phys. B: At. Mol. Opt. Phys.* **46** 224021
[19] Wong M T C and Law C K 2011 *Phys. Rev. A* **83** 055802
[20] Lei S and Lee R 2008 *Phys. Rev. A* **77** 033827
[21] Wang Y, Su Y, Chen X and Wu C 2020 *Phys. Rev. Appl.* **14** 044043
[22] O'Conner K M and Wooters W K 2001 *Phys. Rev. A* **63** 052302
[23] Gunlycke D, Kendon V M and Vedral V 2001 *Phys. Rev. A* **64** 042302
[24] Bose S, Fuentes-Guridi I, Knight P L and Vedral V 2001 *Phys. Rev. Lett.* **87** 050401
[25] Arnesen M C, Bose S and Vedral V 2001 *Phys. Rev. Lett.* **87** 017901
[26] Andrianov S N and Moiseev S A 2014 *Phys. Rev. A* **90** 042303
[27] Goryachev M, Farr W G, Creedon D L, Fan Y, Kostylev M and Tobar M E 2014 *Phys. Rev. Appl.* **2** 054002
[28] Wolski S P, Lachance-Quirion D, Tabuchi Y, Kono S, Noguchi A, Usami K and Nakamura Y 2020 *Phys. Rev. Lett.* **125** 117701
[29] Liu Z, Xiong H and Wu Y 2019 *Phys. Rev. B* **100** 134421
[30] Xie Q, Zhong H, Batchelor M T and Lee C 2017 *J. Phys. A: Math. Theor.* **50** 113001
[31] Pedernales J S, Lizuain I, Felicetti S, Romero G, Lamata L and Solano E 2015 *Sci. Rep.* **5** 15472